Dynamic Model and Control of a Microgrid with Passive Loads

M. Popov, H. Karimi, H. Nikkhajoei, V. Terzija

Abstract **- This paper presents an EMTP control scheme for microgrids with passive loads. The control scheme design is based on a detailed dynamic model of a microgrid. In the dynamic model, the source is represented by a constant voltage source connected in series with an impedance to the voltage-sourced converter. The converter is controlled through a single-input single-output control system. For the grid-connected operation mode, a current-controlled scheme, based on *d-q* variables, was used for the converter input regulation. The converter input current is controlled using Notch Filters and Phased Locked Loop blocks. For the microgrid island operation mode, the converter is controlled in the voltage-controlled mode. The new control scheme and the overall microgrid system are simulated in the ATPDraw software environment. The results obtained demonstrated the effectiveness of the proposed control scheme in providing a desirable dynamic performance for both the grid-connected and islanded operation modes of the microgrid.**

Keywords: **Microgrid, Voltage-Sourced Converter, ATPDraw, Islanded system, Grid-connected system.**

I. Introduction

DISTRIBUTED generation (DG), defined as small-scale electricity generation, is a new concept which is considered as a solution for addressing technical, economical and environmental issues of conventional power systems. The application of DG is under extensive studies and experimental tests. It is recognized, that these are a number of technical challenges concerning the operation, monitoring, control and protection of new DG systems. A systematic approach to consider the emerging potential of DG is to take a system approach, which views generation and associated loads as a subsystem, or a "microgrid" [1], [2]. In general, a microgrid can operate as a *grid-connected system* or as an *island*. However, utilities and existing standards [3],[4] currently do not allow the islanding operation of microgrids. The main reasons are safety concerns related to the energized part of utility system during islanding. However, exceptions are allowed when the island does not include any part of the utility system. For a microgrid used for both the grid-connected and islanded operation, one of the major technical concerns is the electromagnetic transients, particularly those during the change from the grid connected to the islanding mode. The technical challenges become even more severe when a microgrid has passive local loads [5].

This paper presents a control scheme of microgrids with passive local loads. By making use of this control scheme, the electromagnetic transients can also be suppressed. It is based on a detailed dynamic network model, which is developed for the overall microgrid including the local loads. The control system, implementing the new control scheme, is so designed that it controls the converter, which interfaces the source to the microgrid in both the voltage- and current-control modes. In this research, one of the critical challenges was to model and simulate the microgrid realistically enough. The overall test system, consisting of a microgrid with local loads, is simulated in the MATLAB-Simulink and the ATPDraw software environment. Using the developed simulation tool, the performance of the new control scheme were thoroughly tested and analyzed, what is systematically presented in the paper.

II. Studied System

The studied microgrid system is shown in Fig. 1. The microgrid is represented by a DC source, connected to a Voltage-Sourced Converter (VSC). The converter is further connected to a step-up transformer through an R-L filter, modeled by R_t and L_t. A local load is connected on the transformer high-voltage side. During the grid-connected mode, the local load is supplied by both the grid and the microgrid. In the islanding mode (the circuit breaker CB from Fig. 1 in the open position), the load is supplied by the microgrid only.

The local load is a parallel RLC load, which has second-order dynamics. Thus, the load voltage regulation in the islanding mode is highly challenging. On the other hand, the VSC is controlled by a control system, which operates in two main modes. During the grid-connected mode, the controller operates in a *current-control mode*, in which it regulates the exchange of active and reactive powers between the microgrid and the external grid. On the other hand, in the islanded operation, the controller operates in a *voltage-control mode*. After islanding, a severe power mismatch can occur, which affects the voltage and frequency conditions in the microgrid. It will be shown, that in the islanding operation, the voltage-control mode is much more effective than the current control one. The design of the corresponding controller is based on a dynamic model of the overall microgrid, including the RLC local load. It will be shown, that the controller responds

M. Popov is with the Delft University of Technology, Faculty of Electrical Engineering, Mathematics and Computer Science, Delft, The Netherlands, M.Popov@tudelft.nl.

H. Karimi is with the Department of Electrical Engineering, Sharif University of Technology, Tehran, Iran, houshang.karimi@sharif.edu.

H. Nikkhajoei is with Al-Ain Univeristy, the Department of Electrical Engineering, United Arab Emirates, nikkhajoei@uaeu.ae.ae.

V. Terzija is with the University of Manchester, Faculty of Electrical and Electronics Engineering, terzija@ieee.org.

Paper submitted to the International Conference on Power Systems Transients (IPST2009) in Kyoto, Japan June 3-6, 2009

properly to the system inherent dynamics/transients, when islanding.

III. Model of Islanded Microgrid

Fig. 1 shows a single line diagram of a microgrid with an RLC local load. The systematic design of a controller for the overall microgrid can be carried out based on the system dynamic model.

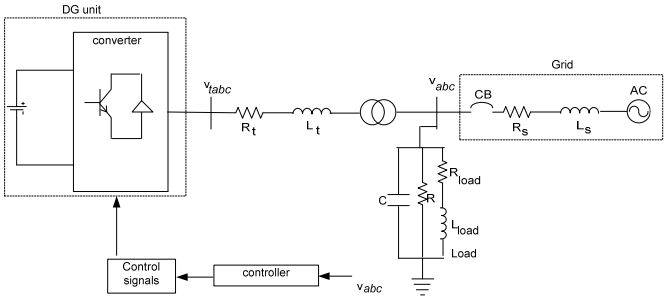

Fig. 1. A microgrid with a RLC local load.

The state-space model of the islanded microgrid is:

$$\begin{aligned} v_{t,abc} &= L_t \frac{di_{t,abc}}{dt} + R_t i_{t,abc} + v_{abc} \\ i_{t,abc} &= C\frac{dv_{abc}}{dt} + i_{L,abc} + \frac{v_{abc}}{R} \\ v_{abc} &= L\frac{di_{L,abc}}{dt} + R_l i_{L,abc} \end{aligned} \tag{1}$$

where v_t and v are terminal voltages from Fig. 1. In equation (1), the *abc* variables represent the phase currents and voltages. Transferring equation (1) to the stationary $\alpha\beta$-reference frame, one obtains:

$$\begin{aligned} \frac{di_{t,\alpha\beta}}{dt} &= -\frac{R_t}{L_t} i_{t,\alpha\beta} - \frac{v_{\alpha\beta}}{L_t} + \frac{v_{t,\alpha\beta}}{L_t} \\ \frac{dv_{\alpha\beta}}{dt} &= \frac{1}{C} i_{t,\alpha\beta} - \frac{1}{RC} v_{\alpha\beta} - \frac{i_{L,\alpha\beta}}{C} \\ \frac{di_{L,\alpha\beta}}{dt} &= \frac{v_{\alpha\beta}}{L} - \frac{R_l}{L} i_{L,\alpha\beta} \end{aligned} \tag{2}$$

Equations (2), transferred to a *dq* rotating reference, become the following form:

$$\begin{aligned} \frac{di_{t,dq}}{dt} + j\omega i_{t,dq} &= -\frac{R_t}{L_t} i_{t,dq} - \frac{v_{dq}}{L_t} + \frac{v_{t,dq}}{L_t} \\ \frac{dv_{dq}}{dt} + j\omega v_{dq} &= \frac{1}{C} i_{t,dq} - \frac{1}{RC} v_{dq} - \frac{i_{L,dq}}{C} \\ \frac{di_{L,dq}}{dt} + j\omega i_{L,dq} &= \frac{v_{dq}}{L} - \frac{R_l}{L} i_{L,dq} \end{aligned} \tag{3}$$

Phase-angle of the load voltage can be selected such that $v_q = 0$. In this case, $\dot{v}_q = 0$ and v_d equals the magnitude of the load voltage. Thus, equations (3) can be rearranged as follows:

$$\begin{aligned} \frac{di_{td}}{dt} &= \omega i_{tq} - \frac{R_t}{L_t} i_{td} - \frac{v_d}{L_t} + \frac{v_{td}}{L_t} \\ \frac{dv_d}{dt} &= \frac{1}{C} i_{td} - \frac{1}{RC} v_d - \frac{i_{Ld}}{C} \\ \frac{di_{Ld}}{dt} &= \omega i_{Lq} + \frac{v_q}{L} - \frac{R_l}{L} i_{Ld} \\ \frac{di_{tq}}{dt} &= -\omega i_{td} - \frac{R_t}{L_t} i_{tq} + \frac{v_{tq}}{L_t} \\ \frac{di_{Lq}}{dt} &= -\omega i_{Ld} - \frac{R_l}{L} i_{Lq} \\ \omega C v_d &= i_{tq} - i_{Lq} \end{aligned} \tag{4}$$

Equations (4) represent the system model in state space variables, which can be shown in the following matrix form:

$$\begin{aligned} X(t) &= AX(t) + bu(t) \\ y(t) &= cX(t) \\ u(t) &= v_{td} \end{aligned} \tag{5}$$

where

$$A = \begin{bmatrix} -\frac{R_t}{L_t} & \omega_0 & 0 & -\frac{1}{L_t} \\ \omega_0 & -\frac{R_t}{L} & -2\omega_0 & \frac{R_l C\omega_0}{L_t} - \frac{\omega_0}{R} \\ 0 & \omega_0 & -\frac{R_l}{L} & \frac{1}{L} - \omega_0^2 C \\ \frac{1}{L} & 0 & -\frac{1}{C} & -\frac{1}{RC} \end{bmatrix} \tag{6}$$

$$b^T = \begin{bmatrix} \frac{1}{L_t} & 0 & 0 & 0 \end{bmatrix}$$

$$c = \begin{bmatrix} 0 & 0 & 0 & 1 \end{bmatrix}$$

$$X^T = \begin{bmatrix} i_{td} & i_{tq} & i_{Lq} & v_d \end{bmatrix}$$

The dynamical model (6) can be readily represented by a Single-Input Single-Output (SISO) transfer function as follows:

$$g(s) = c(sI - A)^{-1} b = \frac{N(s)}{D(s)} \tag{7}$$

where

$$\begin{aligned} N(s) &= RL^2\left(s^2 + \frac{2R_l}{L}s + \frac{\omega_0^2 L^2 + R_l^2}{L^2}\right) \\ D(s) &= a_4 s^4 + a_3 s^3 + a_2 s^2 + a_1 s + a_0 \end{aligned} \tag{8}$$

a_i, i=0, 1, 2, 3 are polynomial functions of the system parameters, expressed as follows:

$$
\begin{aligned}
a_4 &= L_t R L^2 C \\
a_3 &= \left(L_t L^2 + R_t R L^2 C + 2 R_l R L C L_t\right) \\
a_2 &= \left(L_t R L + R L^2 + R_t L^2 + 2 R_l R_t R C L + 2 R_l L_t L + L_t R C R_l^2\right) \\
a_1 &= R_t R L + 2 R_l R L + R_t R_l^2 R C + 2 R_l R_t L + R_t R L^2 C \omega_0^2 + L_t R_l^2 \\
&\quad + L_t L^2 \omega_0^2 - 2 R_l R L C \omega_0^2 L_t \\
a_0 &= R_t R_l R + R L^2 \omega_0^2 + R_t L^2 \omega_0^2 + R_l^2 R + R_l^2 R_t + R L \omega_0^2 L_t - \\
&\quad R_l^2 R C \omega_0^2 L_t - R L^2 C \omega_0^4 L_t
\end{aligned}
\tag{9}
$$

In [5] the control strategy for an islanded microgrid is described. Fig. 2 shows a block diagram of the Phase-Locked Loop (PLL), used n the converter control system. The voltages v_{abc} are transformed to the *dq* frame so that v_q is zero. The output signal v_d is compared with the corresponding reference $v_{d,ref}$ and the resultant error is given to the controller F(s). The controller is designed using MATLAB Control Toolbox. Placing one of the poles at the origin, the other real pole will be at -100. The gain is tuned until a desired overshoot and zero steady-state error are obtained. For the designed control system, the controller $F(s)$ has the following transfer function:

$$
F(s) = \frac{4000}{s(s+100)}. \tag{10}
$$

The three-phase PLL estimates the phase-angle $\theta(t)$ at the common coupling point for the grid-connected operation. In the islanding operation mode, a crystal oscillator is employed to regulate the island frequency in an open-loop manner.

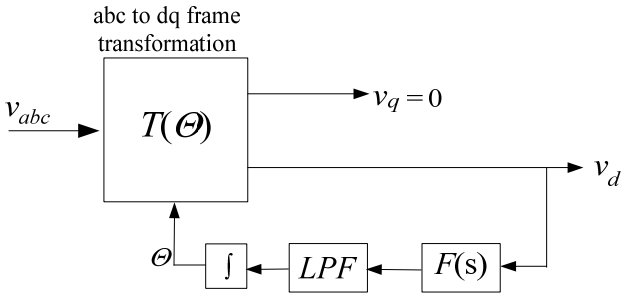

Fig. 2. Block diagram of the embedded PLL.

IV. Model of Grid-Connected Microgrid

For the grid-connected operation, a *current-control method* is applied. The load voltages v_{abc} are measured and transferred to the *dq* frame. Using a PLL, the phase-angle θ at the common coupling point is estimated and used to generate the *dq* quantities. Fig. 2 shows the designed PLL [6]. It is also explained in [7]. The current-control method is described in Fig. 3 [8]. The control voltages $v_{t,dq}$ are transformed to the *abc* variables, which proceed to the PWM block to generate the gating signals for the converter. The detailed controller block of Fig. 3 is shown in Fig. 4. The PI controllers are designed using MATLAB SISO tools so that the desired dynamic performance indices are met.

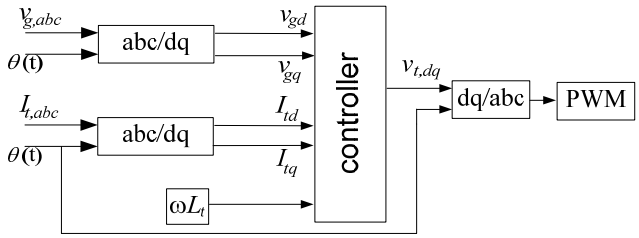

Fig. 3. Block diagram of the converter control system.

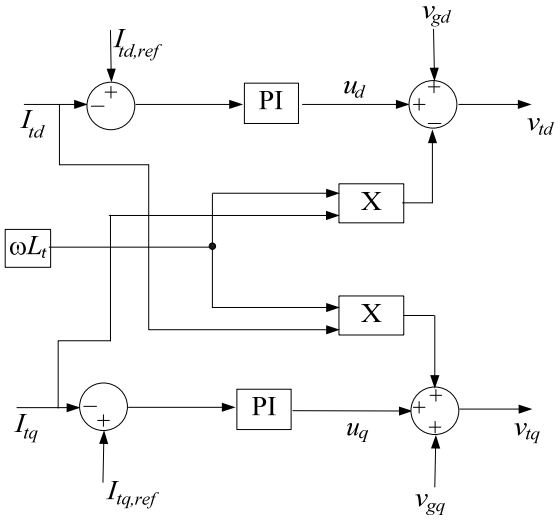

Fig. 4. Details of the controller block from Fig. 3.

V. ATP-EMTP Model

The control methods for the islanded and grid-connected microgrid have been modeled and simulated in the MATLAB-Simulink and ATPDraw environment. In this Section only the ATPDraw model will be explained. Fig. 5 shows the ATPDraw model of the microgrid of Fig. 1. The microgrid is modeled with the available power system components of the ATP-EMTP. The converter control is implemented based on the models described in Fig. 3 and Fig. 4. The converter is represented by six ideal type-13 switches in the ATP-EMTP. The control outputs, Fig. 3, are given to a PWM block that generates gating signals for the IGBT switches of the converter. The described ATPDraw model can implement multiple modes and control strategies requires for simulating the microgrid for both the islanded and the grid-connected operation.

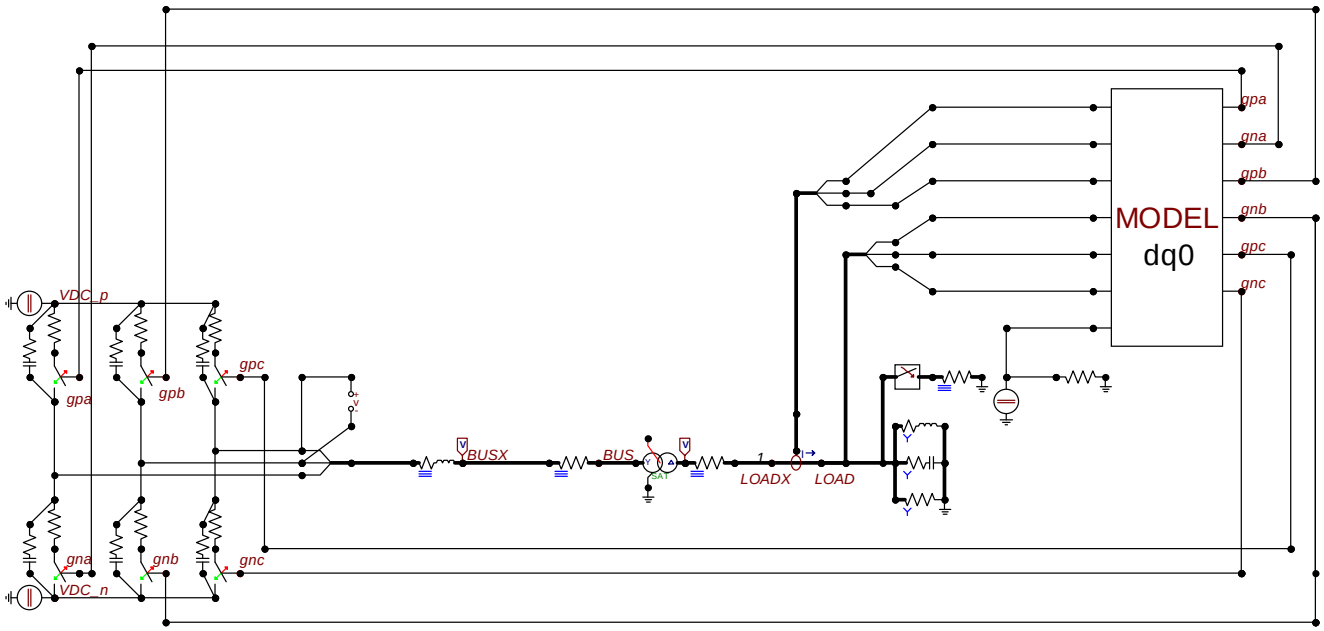

Fig. 5. ATP model of the microgrid of Fig. 1.

VI. Simulation Results

A. Islanded Operation

During islanded mode of operation, a few examples have been done in order to investigate the performance of the controller to sudden changes within an islanded network.

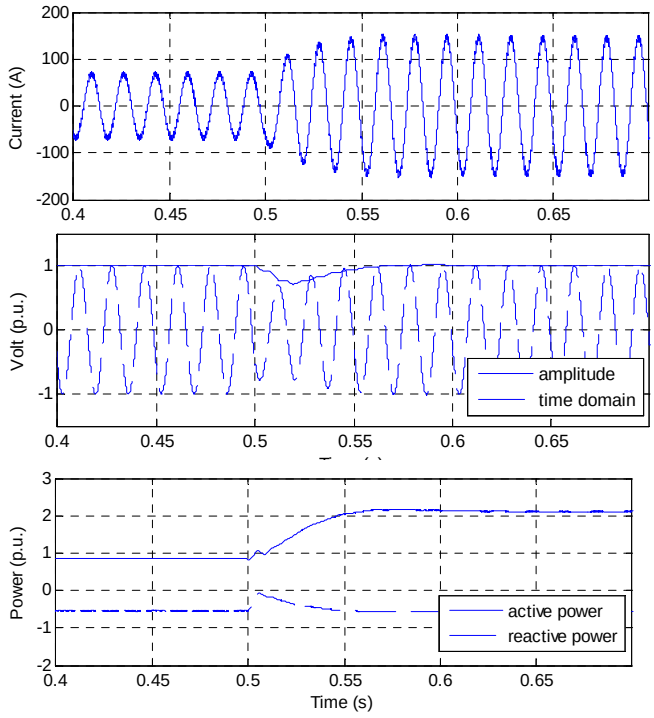

Fig. 6. Dynamic performance of the islanded microgrid of Fig. 1 for a load step increase: load current (upper graph); load voltage (middle graph); and load real and reactive powers (lower graph).

Fig. 6 shows dynamic performance of the islanded microgrid of Fig. 1 operating with the designed control system for a step increase in the local load. The microgrid is initially operating in steady state, and at t = 0.5 seconds the load resistance, inductance and capacitance are changed. The microgrid reaches to a new steady-state operating point after about three cycles which indicate the effective response of the designed control system. Variations of the load current and voltage and the load active and reactive power components are shown in Fig. 6.

Fig. 7 shows dynamic performance of the islanded microgrid from Fig. 1 operating with the designed control system for a change in the load voltage reference. The microgrid is initially

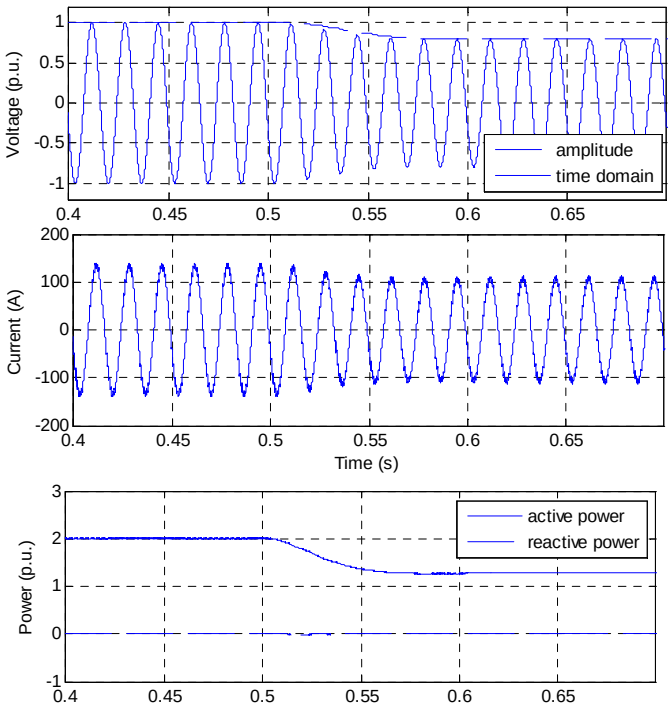

Fig. 7. Dynamic performance of the islanded microgrid of Fig. 1 for a change in the load voltage reference: load voltage (upper graph); load current (middle graph); and load real and reactive powers (lower graph).

operating in steady state, and at t = 0.5 seconds the load voltage reference is changed. The microgrid reaches to a new steady-state operating point after about four cycles which indicate the effective response of the designed control system. Variations of the load voltage and current and the load real and reactive power components are shown in Fig. 7.

B. Grid-connected Operation

This section evaluates dynamic performance of the grid-connected microgrid of Fig. 1 when operating with the designed control system. Fig. 8 and Fig. 9 show dynamic performance of the grid-connected microgrid of Fig. 1 for changes in the microgrid real and reactive (*dq*) current references. The system initially operates in steady state with no real/reactive powers from the microgrid. The references of I_d and I_q are changes at t=0.5 s and t=0.7 to 1000 A and 500 A, respectively. Variations of the microgrid *dq* current components, the grid phase current, the grid real and reactive powers and the converter output voltage are shown in Fig. 8. The results demonstrate that the designed control system effectively and smoothly transfers the overall system to the new operating conditions.

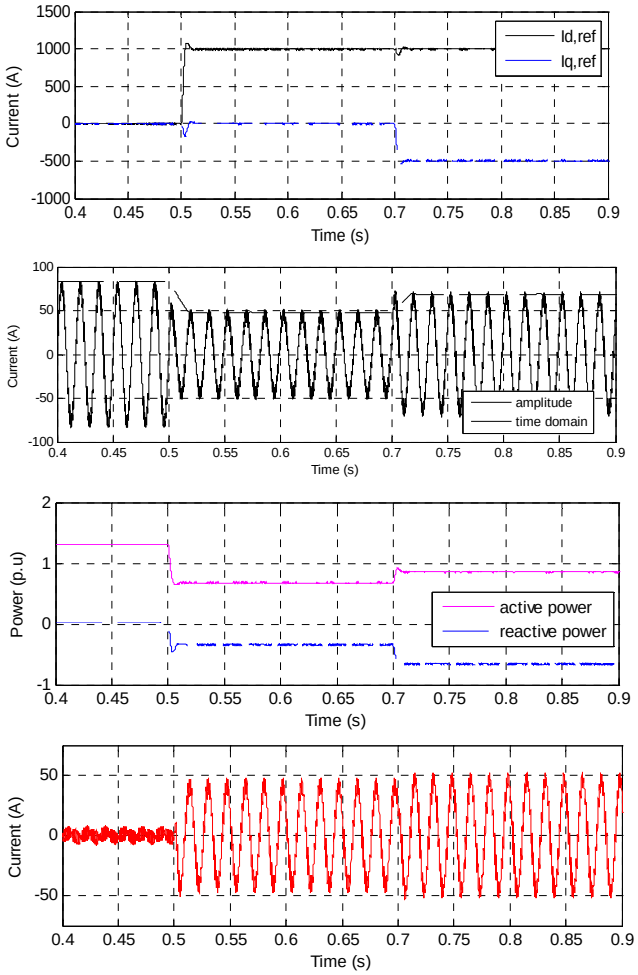

Fig. 8. Dynamic performance of the grid-connected microgrid of Fig. 1 for changes in the microgrid real and reactive (*dq*) current references: microgrid dq current components; grid phase current; grid real and reactive powers; converter output current.

Fig. 9 shows the converter terminal phases a, b and c, and line-to-line voltages corresponding to the operating conditions from Fig. 8.

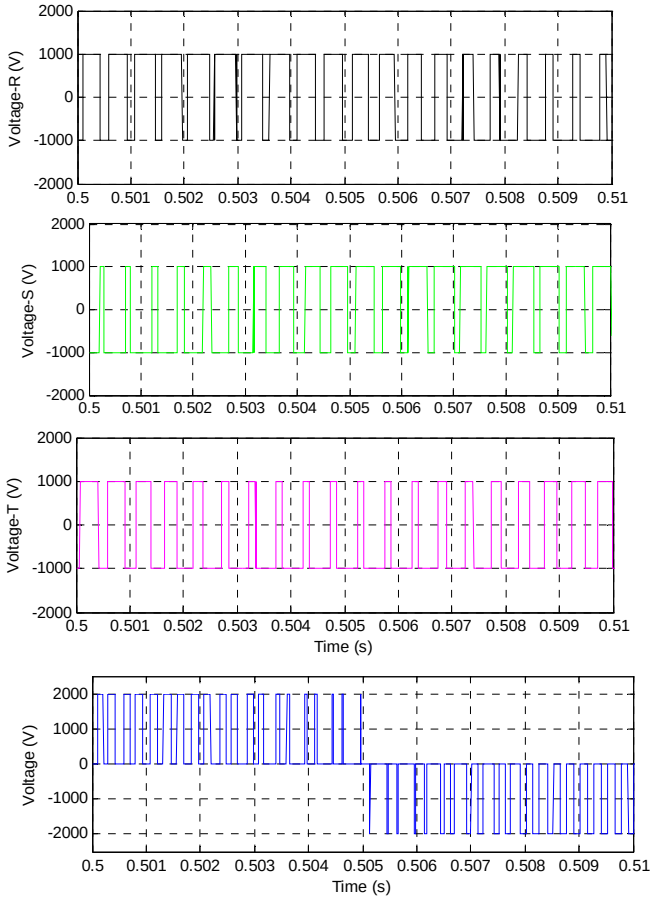

Fig. 9. Same as Fig. 8: converter phase a, b, and c voltages (first three graphs); and converter line-to-line voltage (fourth graph).

VII. Discussions

It should be noted that the proposed controller is a fixed controller, i.e., it is not an adaptive controller in which the controller's parameters are tuned based on the estimation of the unknown parameters. Basically, the authors believe that the adaptive control is not a reliable approach to be used in the power electronics/systems applications.

The performance of the proposed controller against the perturbations in the load parameters and with respect to the transition from the grid-connected mode to the islanded mode was investigated in [5]. Moreover, a laboratory scale test system was implemented in the ECE Department of the University of Toronto to experimentally verify the performance of the controller. The experimental results including a robust stability analysis of the closed-loop system will be the subject of an ongoing paper.

VIII. Conclusions

A systematic control design was presented for a microgrid with passive local loads. The control design is based on a dynamic model that is developed for the overall microgrid

including the local load. To operate the microgrid as an island, a voltage-control method is employed vs. a current-control one which is used for the grid-connected operation. Based on a transfer function of the microgrid obtained from the developed dynamic model, a control system is designed using MATLAB toolbox. The overall microgrid is modeled in the ATPDraw software environment. Performance of the microgrid and the designed control system is evaluated based on digital time-domain simulations for both the grid-connected and islanded operations. The results demonstrate effectiveness of the designed control system in suppressing the system transients when subject to large disturbances.

IX. Future work

The presented method will be implemented in a Real-Time Digital Simulator at TU Delft where the Laboratory of Renewable Energy including two motor-generator sets and solar panels will serve as a microgrid.

X. Appendix

Parameters of the System from Fig. 1:
V_{dc} = 1000 V, f = 60 Hz, f_{sw} = 1980 Hz
R = 76 Ω, C = 62.855 μF, R_{load} = 0.4 Ω, L_{load} = 0.111 H
R_t = 0.15 mΩ, L_t = 0.3 mH, R_s=1 Ω, L_s=10 mH.

XI. References

[1] P. Piagi, and R.H. Lasseter, "Autonomous Control of Microgrids," *Presented at the IEEE Power Eng. Soc. General Meeting*, Montreal, QC, Canada, June 18-22, 2006.

[2] S. M. Amin and B. F. Wollenberg, "Toward a smart grid: Power Delivery for the 21st century," *IEEE Power Energy Mag.*, Vol. 3, No. 5, pp. 34-41, September/October 2005.

[3] "Standard Conformance Test Procedures for Equipment Interconnecting Distributed Resources with Electric Power Systems," *IEEE Std. 1547.1*, 2005.

[4] "Inverters, Converters and Controllers for Use in Independent Power Systems," *UL Std. 1741*, 2002.

[5] H. Karimi, H. Nikkhajoei, R. Iravani, "Control of an Electronically-Coupled Distributed Resource Unit Subsequent to an Islanding Event," *IEEE Trans. on Power Delivery*, Vol. 23, No. 1, pp. 493-501, January 2008.

[6] A. Yazdani, R. Iravani, "A Unified Dynamic Control for the Voltage-Sourced Converter Under Unbalanced Grid Conditions," *IEEE Trans. on Power Delivery*, Vol. 21, No. 3, pp. 1620-1629, July 2006.

[7] D. Jovcic, "Phase Locked Loop System for FACTS", *IEEE Trans. on Power Systems*, Vol. 18, No. 3, pp. 1116-1123, August 2003.

[8] G. Schauder, H. Mehta, "Vector Analysis and Control of Advanced Static VAR compensators," *IEE Proceedings-C*, Vol. 140, No. 4, pp. 299-306, July 1993.